Antitumor activities of a defucosylated anti-EpCAM monoclonal antibody in colorectal carcinoma xenograft models

GUANJIE LI[1*], HIROYUKI SUZUKI[1*], TOMOKAZU OHISHI[2*], TEIZO ASANO[3], TOMOHIRO TANAKA[3], MIYUKI YANAKA[3], TAKURO NAKAMURA[3], TAKEO YOSHIKAWA[4], MANABU KAWADA[2], MIKA K. KANEKO[3] and YUKINARI KATO[1,3,4]

[1]Department of Molecular Pharmacology, Tohoku University Graduate School of Medicine, Sendai, Miyagi 980-8575; [2]Institute of Microbial Chemistry (BIKAKEN), Microbial Chemistry Research Foundation, Numazu, Shizuoka 410-0301; Departments of [3]Antibody Drug Development and [4]Pharmacology, Tohoku University Graduate School of Medicine, Sendai, Miyagi 980-8575, Japan

Received August 14, 2022; Accepted December 7, 2022

DOI: 10.3892/ijmm.2023.5221

Abstract. Epithelial cell adhesion molecule (EpCAM) is a type I transmembrane glycoprotein, which is highly expressed on tumor cells. As EpCAM plays a crucial role in cell adhesion, survival, proliferation, stemness, and tumorigenesis, it has been considered as a promising target for tumor diagnosis and therapy. Anti-EpCAM monoclonal antibodies (mAbs) have been developed and have previously demonstrated promising outcomes in several clinical trials. An anti-EpCAM mAb, EpMab-37 (mouse IgG_1, kappa) was previously developed by the authors, using the cell-based immunization and screening method. In the present study, a defucosylated version of anti-EpCAM mAb (EpMab-37-mG_{2a}-f) was generated to evaluate the antitumor activity against EpCAM-positive cells. EpMab-37-mG_{2a}-f recognized EpCAM-overexpressing CHO-K1 (CHO/EpCAM) cells with a moderate binding-affinity [dissociation constant (K_D)=2.2x10^{-8} M] using flow cytometry. EpMab-37-mG_{2a}-f exhibited potent antibody-dependent cellular cytotoxicity (ADCC) and complement-dependent cytotoxicity (CDC) for CHO/EpCAM cells by murine splenocytes and complements, respectively. Furthermore, the administration of EpMab-37-mG_{2a}-f significantly suppressed CHO/EpCAM xenograft tumor development compared with the control mouse IgG. EpMab-37-mG_{2a}-f also exhibited a moderate binding-affinity (K_D=1.5x10^{-8} M) and high ADCC and CDC activities for a colorectal cancer cell line (Caco-2 cells). The administration of EpMab-37-mG_{2a}-f to Caco-2 tumor-bearing mice significantly suppressed tumor development compared with the control. By contrast, EpMab-37-mG_{2a}-f never suppressed the xenograft tumor growth of Caco-2 cells in which EpCAM was knocked out. On the whole, these results indicate that EpMab-37-mG_{2a}-f may exert antitumor activities against EpCAM-positive cancers and may thus be a promising therapeutic regimen for colorectal cancer.

Correspondence to: Dr Hiroyuki Suzuki or Dr Yukinari Kato, Department of Molecular Pharmacology, Tohoku University Graduate School of Medicine, 2-1 Seiryo-machi, Aoba-ku, Sendai, Miyagi 980-8575, Japan
E-mail: hiroyuki.suzuki.b4@tohoku.ac.jp
E-mail: yukinari.kato.e6@tohoku.ac.jp

*Contributed equally

Abbreviations: EpCAM, epithelial cell adhesion molecule; mAb, monoclonal antibody; ADCC, antibody-dependent cellular cytotoxicity; CDC, complement-dependent cytotoxicity; FDA, Food and Drug Administration; FcγR, Fcγ receptor; NK, natural killer; RPMI, Roswell Park Memorial Institute; PBS, phosphate-buffered saline; K_D, dissociation constant

Key words: EpCAM monoclonal antibody, ADCC, CDC, colorectal cancer

Introduction

Epithelial cell adhesion molecule (EpCAM) is expressed on the basolateral membrane of epithelial cells (1). EpCAM is a unique type I transmembrane glycoprotein which possesses a different structure and functions compared to other classical adhesion molecules, including cadherins, selectins and integrins. EpCAM-mediated homophilic and intercellular adhesion are essential for the maintenance of the epithelial integrity (2). EpCAM also plays critical roles in intercellular signaling. Following the cleavage of the EpCAM intracellular domain, it functions as a transcriptional co-factor with β-catenin and regulates the transcriptional targets involved in cell proliferation, survival and stemness (3). Therefore, the overexpression of EpCAM plays a key role in tumor development.

EpCAM is a critical marker for the isolation circulating tumor cells (CTCs). CTCs provide critical prognostic information as an indicator of micro-metastasis, and determine the response to some cancer therapeutics (4). The US Food and Drug Administration (FDA) confirmed the clinical importance of CTCs, and approved of CellSearch®, a platform that can be used for the isolation of EpCAM-positive, CD45-negative cells

from whole blood samples (5). The EpCAM-based CellSearch® CTC test has been studied in several clinical trials in lung (6), breast (7) and prostate (8) cancers.

Therapeutic monoclonal antibodies (mAbs) are the most crucial biological therapeutics for the treatment of various tumors (9) and inflammatory diseases, such as rheumatoid arthritis (10). EpCAM was the first identified human tumor-associated antigen, and plays a critical role in tumor development (11). Therefore, EpCAM has been considered as a target of mAb therapies, including Adecatumumab (12) and Edrecolomab (13,14) in EpCAM-overexpressing breast, prostate, gastrointestinal and colorectal cancers. A humanized single chain Fv against EpCAM, fused to *Pseudomonas* exotoxin A, Oportuzumab monatox, has been evaluated in bladder cancer, as have been previously reviewed (15). A bispecific EpCAM/CD3-antibody, Catumaxomab, functions as the trifunctional antibody. When Catumaxomab recognizes EpCAM-high tumors, it also recruits T-cells to tumors. This event promotes the formation of cytotoxic synapse and T-cell-mediated cytotoxicity. Furthermore, Catumaxomab recruits natural killer (NK) cells and macrophages through the Fc domain and enhances antibody-dependent cellular cytotoxicity (ADCC) (16,17). Catumaxomab has demonstrated promising outcomes in several clinical trials (18-20), and has been approved by the European Union for the treatment of patients with malignant ascites (21).

ADCC is mediated by NK cells upon the binding of the FcγRIIIa to the Fc region of mAbs. The FcγRIIIa engagement can stimulate NK cells, which attack and lyse target cells (9). However, this function is affected by the *N*-linked glycosylation in the Fc region (22). In particular, a core fucose deficiency on the Fc *N*-glycan has been revealed to enhance the Fc binding to the FcγRIIIa on the effector cells (23). In a previous study on recombinant mAb production using Chinese hamster ovary (CHO) cells, the Fc *N*-glycans were determined as an heterogeneous biantennary complex (22). Fucosyltransferase 8 (FUT8) is the only α1,6-fucosyltransferase transferring fucose via an α1,6 linkage to the innermost *N*-acetylglucosamine on *N*-glycans for core fucosylation. CHO cells subjected to FUT8 knockout have been revealed to produce completely defucosylated recombinant antibodies. Furthermore, mAb produced by CHO cells subjected to FUT8 knockout strongly binds to FcγRIIIa and potently enhances ADCC activity compared to mAb produced by wild-type CHO. Therefore, CHO cells subjected to FUT8 knockout may be an ideal host cell for the production of completely defucosylated high-ADCC mAb for therapeutic use (24).

An anti-EpCAM mAb, EpMab-37 (mouse IgG_1, kappa) has been previously established by the authors, using the cell-based immunization and screening method (25). In the present study, a defucosylated anti-EpCAM mAb (EpMab-37-mG_{2a}-f) was produced by using FUT8-deficient CHO cells to potentiate antitumor activity and investigated the ability of EpMab-37-mG_{2a}-f to induce ADCC, complement-dependent cytotoxicity (CDC) and antitumor activity in EpCAM-expressing cells.

Materials and methods

Cell lines and cell culture. CHO-K1 (ATCC CCL-61) and the human colorectal cancer cell lines, Caco-2 (ATCC HTB-37), HCT116 (ATCC CCL-247), HT-29 (ATCC HTB-38), LS174T (ATCC CL-188), COLO201 (ATCC CCL-224), HCT-8 (ATCC CCL-244) and SW1116 (ATCC CCL-233), were purchased from the ATCC. HCT-15 (TKG 0504), COLO205 (TKG 0457) and DLD-1 (TKG 0379) were purchased from the Cell Resource Center for Biomedical Research Institute of Development, Aging and Cancer at Tohoku University. EpCAM cDNA plus a C-terminal PA tag (EpCAM-PA) was subcloned into a pCAG-Ble vector (FUJIFILM Wako Pure Chemical Corporation). CHO/EpCAM was established by transfecting the pCAG/EpCAM-PA vector into CHO-K1 cells using the Neon Transfection System (Thermo Fisher Scientific, Inc.). CHO-K1 cells ($1.5x10^6$) were transfected with the pCAG/EpCAM-PA vector. Positive cells for anti-EpCAM mAb (clone 9C4; cat. no. 324202; BioLegend, Inc.) were sorted using an SH800 cell sorter (Sony Corporation) and selected as previously described (26,27). CHO-K1 and CHO/EpCAM cells were cultured in Roswell Park Memorial Institute (RPMI)-1640 medium (Nacalai Tesque, Inc.), supplemented with 10% heat-inactivated fetal bovine serum (FBS; Thermo Fisher Scientific, Inc.), 100 U/ml penicillin, 100 μg/ml streptomycin and 0.25 μg/ml amphotericin B (Nacalai Tesque, Inc.). Caco-2 cells and Caco-2 cells in which EpCAM was knocked out (BINDS-16), which were previously established (26), were cultured in DMEM (Nacalai Tesque, Inc.), supplemented with 10% FBS, 100 units/ml penicillin and 100 μg/ml streptomycin. The COLO201, COLO205, SW1116 and DLD-1 cells were cultured in RPMI-1640 medium (Nacalai Tesque, Inc.), supplemented with 10% FBS, 100 units/ml penicillin and 100 μg/ml streptomycin (Nacalai Tesque, Inc.). The HCT116, HT-29, LS174T and HCT-8 were cultured in DMEM (Nacalai Tesque, Inc.), supplemented with 10% FBS, 100 U/ml penicillin and 100 μg/ml streptomycin. All cell lines were maintained at 37˚C in a humidified atmosphere under 5% CO_2.

Animal experiments. All animal experiments were performed following regulations and guidelines to minimize animal distress and suffering in the laboratory by the Institutional Committee for Experiments of the Institute of Microbial Chemistry (Numazu, Japan). The animal study protocol was approved (approval no. 2022-024) by the Institutional Committee for Experiments of the Institute of Microbial Chemistry (Numazu, Japan). BALB/c nude mice (female, a total of 70 mice) were maintained on an 11-h light/13-h dark cycle in a specific pathogen-free environment, across the experimental period. Food and water were supplied *ad libitum*. The weight of the mice was monitored twice per week and their health was monitored three times per week. The loss of original body weight was determined to a point >25% (28) and/or a maximum tumor size >3,000 mm^3 and/or significant changes in the appearance of tumors as humane endpoints for euthanasia. Cervical dislocation was used for euthanasia. Mouse death was confirmed by respiratory arrest and rigor mortis.

Antibodies. Anti-EpCAM mAb, EpMab-37 was previously established (25). To generate recombinant EpMab-37, V_H cDNA of EpMab-37 and C_H of mouse IgG_{2a} was cloned into the pCAG-Ble vector. V_L cDNA of EpMab-37 and C_L

cDNA of mouse kappa light chain were also subcloned into the pCAG-Neo vector (FUJIFILM Wako Pure Chemical Corporation). The vector for the recombinant EpMab-37 was transduced into BINDS-09 (FUT8-knockout ExpiCHO-S) cells using the ExpiCHO Expression System (Thermo Fisher Scientific, Inc.), as previously described (29-36). EpMab-37-mG_{2a}-f was purified using Ab-Capcher (ProteNova Co., Ltd.). Mouse IgG (cat. no. 140-09511) and IgG_{2a} (cat. no. M7769) were purchased from FUJIFILM Wako Pure Chemical Corporation and MilliporeSigma, respectively. 281-mG_{2a}-f [defucosylated anti-hamster podoplanin (PDPN) mAb, control mouse IgG_{2a} for ADCC reporter bioassay] was previously described (37).

Flow cytometry. CHO-K1, CHO/EpCAM and Caco-2 cells were isolated using 0.25% trypsin and 1 mM ethylenediamine tetraacetic acid (EDTA; Nacalai Tesque, Inc.) treatment. The cells were treated with EpMab-37-mG_{2a}-f, or blocking buffer [0.1% bovine serum albumin (BSA; Nacalai Tesque, Inc.) in phosphate-buffered saline (PBS)] (control) for 30 min at 4˚C. Subsequently, the cells were incubated in Alexa Fluor 488-conjugated anti-mouse IgG (1:2,000; cat. no. 4408; Cell Signaling Technology, Inc.) for 30 min at 4˚C. Fluorescence data were collected using the SA3800 Cell Analyzer and analyzed using SA3800 software ver. 2.05 (Sony Corporation).

Determination of binding affinity. Serially diluted EpMab-37-mG_{2a}-f (0.006-100 μg/ml) was suspended with CHO/EpCAM and Caco-2 cells. The cells were further treated with Alexa Fluor 488-conjugated anti-mouse IgG (1:200). Fluorescence data were collected using BD FACSLyric and analyzed using BD FACSuite software version 1.3 (BD Biosciences). To determine the dissociation constant (K_D), GraphPad Prism 8 (the fitting binding isotherms to built-in one-site binding models; GraphPad Software, Inc.) was used.

ADCC of EpMab-37-mG_{2a}-f. ADCC induction by EpMab-37-mG_{2a}-f was assayed as follows: Six female BALB/c nude mice (5 weeks old) were purchased from Charles River Laboratories, Inc. The spleens were aseptically removed and single-cell suspensions were obtained through a sterile cell strainer (cat. no. 352360; BD Falcon). Erythrocytes were removed with the treatment of ice-cold distilled water. The splenocytes were resuspended in DMEM with 10% FBS; this preparation was designated as effector cells. Target cells (CHO-K1, CHO/EpCAM and Caco-2) were treated with 10 μg/ml Calcein AM (Thermo Fisher Scientific, Inc.) (38). The target cells ($2x10^4$ cells) were plated in 96-well plates and mixed with effector cells (effector-to-target ratio, 100:1), 100 μg/ml of EpMab-37-mG_{2a}-f or control mouse IgG_{2a}. Following incubation for 4.5 h at 37˚C, the Calcein release into the medium was measured with an excitation wavelength (485 nm) and an emission wavelength (538 nm) using a microplate reader (Power Scan HT; BioTek Instruments, Inc.).

The total percentage of cell lysis was determined as follows: % lysis=(E-S)/(M-S) x100, where 'E' corresponds to the fluorescence in the presence of both effector and target cells, 'S' to the spontaneous fluorescence in the presence of only target cells and 'M' to the maximum fluorescence by the treatment with a lysis buffer [10 mM Tris-HCl (pH 7.4), 10 mM of EDTA and 0.5% Triton X-100].

CDC of EpMab-37-mG_{2a}-f. Target cells (CHO-K1, CHO/EpCAM and Caco-2) were treated with 10 μg/ml Calcein AM (39). The target cells ($2x10^4$ cells) were mixed with rabbit complement (final dilution 1:10; Low-Tox-M Rabbit Complement; Cedarlane Laboratories) and 100 μg/ml control mouse IgG_{2a} or EpMab-37-mG_{2a}-f. Following incubation for 4.5 h at 37˚C, Calcein release into the medium was measured.

ADCC reporter bioassay. The ADCC reporter bioassay was performed using an ADCC Reporter Bioassay kit (cat. no. G7018; Promega Corporation), according to the manufacturer's instructions (40). Target cells (12,500 cells per well) were inoculated into a 96-well white solid plate (cat. no. 655083; Greiner Bio-One). EpMab-37-mG_{2a}-f, EpMab-37 and 281-mG_{2a}-f were serially diluted and added to target cells. Jurkat cells (a component of ADCC Reporter Bioassay kit) stably expressing the human FcγRIIIa receptor, and a nuclear factor of activated T-cells (NFAT) response element driving Firefly luciferase, were used as effector cells. The engineered Jurkat cells (75,000 cells in 25 μl) were then added and co-cultured with antibody-treated target cells at 37˚C for 6 h. Luminescence using the Bio-Glo Luciferase Assay System was measured with a GloMax luminometer (Promega Corporation).

Antitumor activity of EpMab-37-mG_{2a}-f in xenografts of CHO-K1 and CHO/EpCAM. BALB/c nude mice (female, 32 mice) were purchased from Charles River Laboratories, Inc. The CHO-K1 and CHO/EpCAM cells ($5x10^6$ cells) suspended with BD Matrigel Matrix Growth Factor Reduced (BD Biosciences) were inoculated into the left flank of the mice subcutaneously. On day 6 after the inoculation, 100 μg EpMab-37-mG_{2a}-f (n=8) or control mouse IgG (n=8) in 100 μl PBS were injected intraperitoneally. Additional antibody injections were performed on day 14. The dose was based on a biodistribution study of mouse-derived anti-EpCAM mAb (MOC31) (41). The tumor volume was measured on days 6, 11, 14, 18 and 20, and determined as previously described (42). On day 18, ulcerations began to appear in some tumors. As ulcerated tumors result in skin breakdown and a decrease in tumor weight, it was decided to terminate the experiment on day 20 prior to the diameter of the ulcers exceeding 4 mm. The health and well-being of the animals did not deteriorate during these 2 days. The xenograft tumors with or without ulceration were carefully removed from the sacrificed mice, and then weighed and photographed immediately.

Antitumor activity of EpMab-37-mG_{2a}-f in xenografts of Caco-2 and BINDS-16 cells. The Caco-2 and BINDS-16 cells ($5x10^6$ cells) resuspended with BD Matrigel Matrix Growth Factor Reduced (BD Biosciences) were inoculated into the left flank of BALB/c nude mice (female, 32 mice) subcutaneously. On day 6 after the inoculation, 100 μg EpMab-37-mG_{2a}-f (n=8) or control mouse IgG (n=8) in 100 μl PBS were injected intraperitoneally. Additional antibody injections were performed on days 14 and 20. The tumor volume was measured on

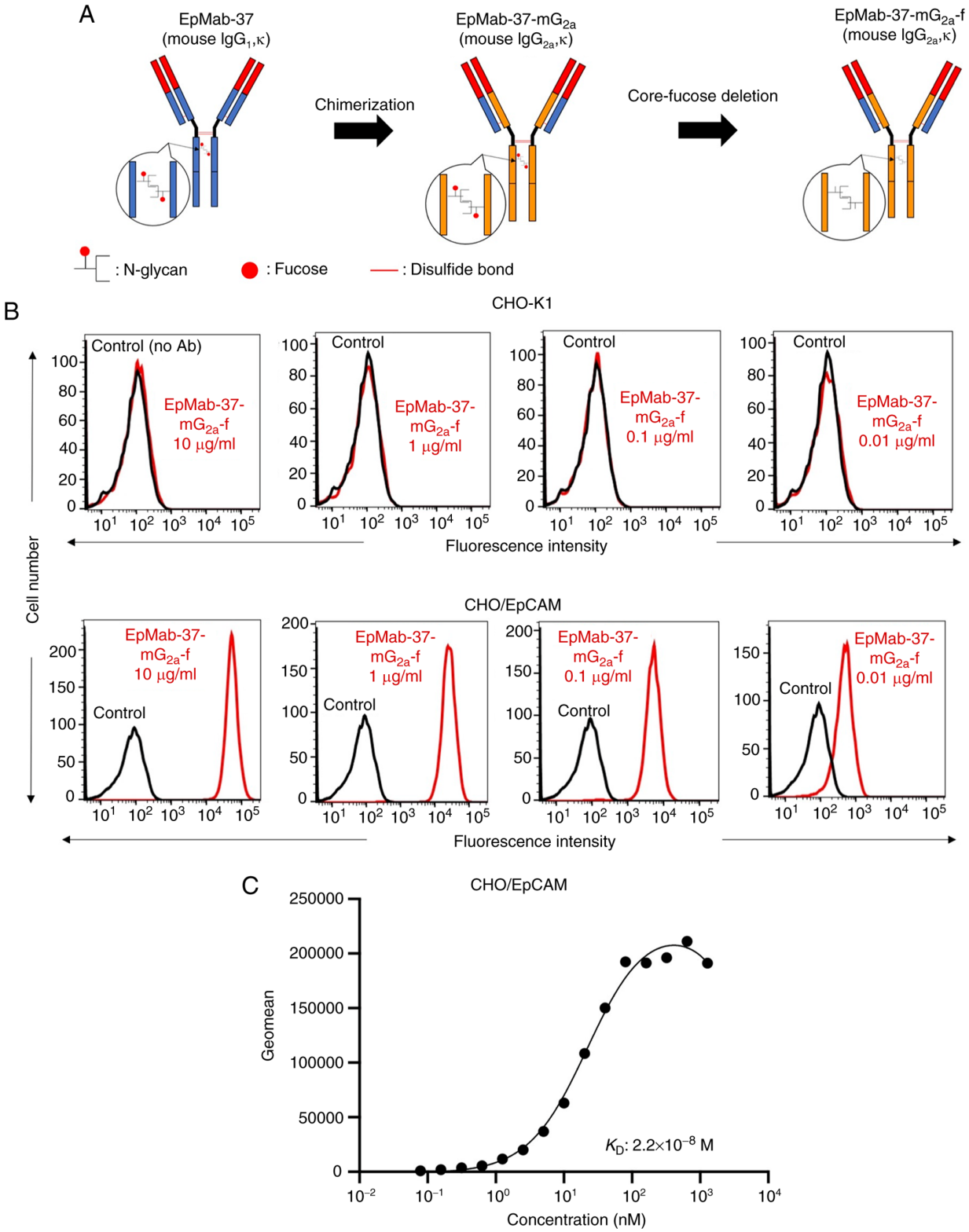

Figure 1. Flow cytometry using EpMab-37-mG$_{2a}$-f. (A) Production of EpMab-37-mG$_{2a}$-f (core-fucose-deficient mouse IgG$_{2a}$) from EpMab-37 (mouse IgG$_1$). (B) CHO-K1 and CHO/EpCAM cells were treated with EpMab-37-mG$_{2a}$-f (red) or buffer control (black), followed by Alexa Fluor 488-conjugated anti-mouse IgG. Fluorescence data were analyzed using the SA3800 Cell Analyzer. (C) Determination of the binding affinity of EpMab-37-mG$_{2a}$-f using flow cytometry for CHO/EpCAM cells. CHO/EpCAM cells were suspended in serially diluted EpMab-37-mG$_{2a}$-f. Alexa Fluor 488-conjugated anti-mouse IgG was then added. Fluorescence data were collected using the BD FACSLyric and the K_D was calculated using GraphPad PRISM 8 software. CHO, Chinese hamster ovary; EpCAM, epithelial cell adhesion molecule; K_D, dissociation constant.

days 6, 11, 14, 18, 20, 25 and 27, and determined as previously described (42). The xenograft tumors were removed, weighed and photographed as described above.

Statistical analyses. All data are expressed as the mean ± standard error of the mean (SEM). In ADCC, CDC and tumor weight measurement, unpaired Welch's t-test was conducted.

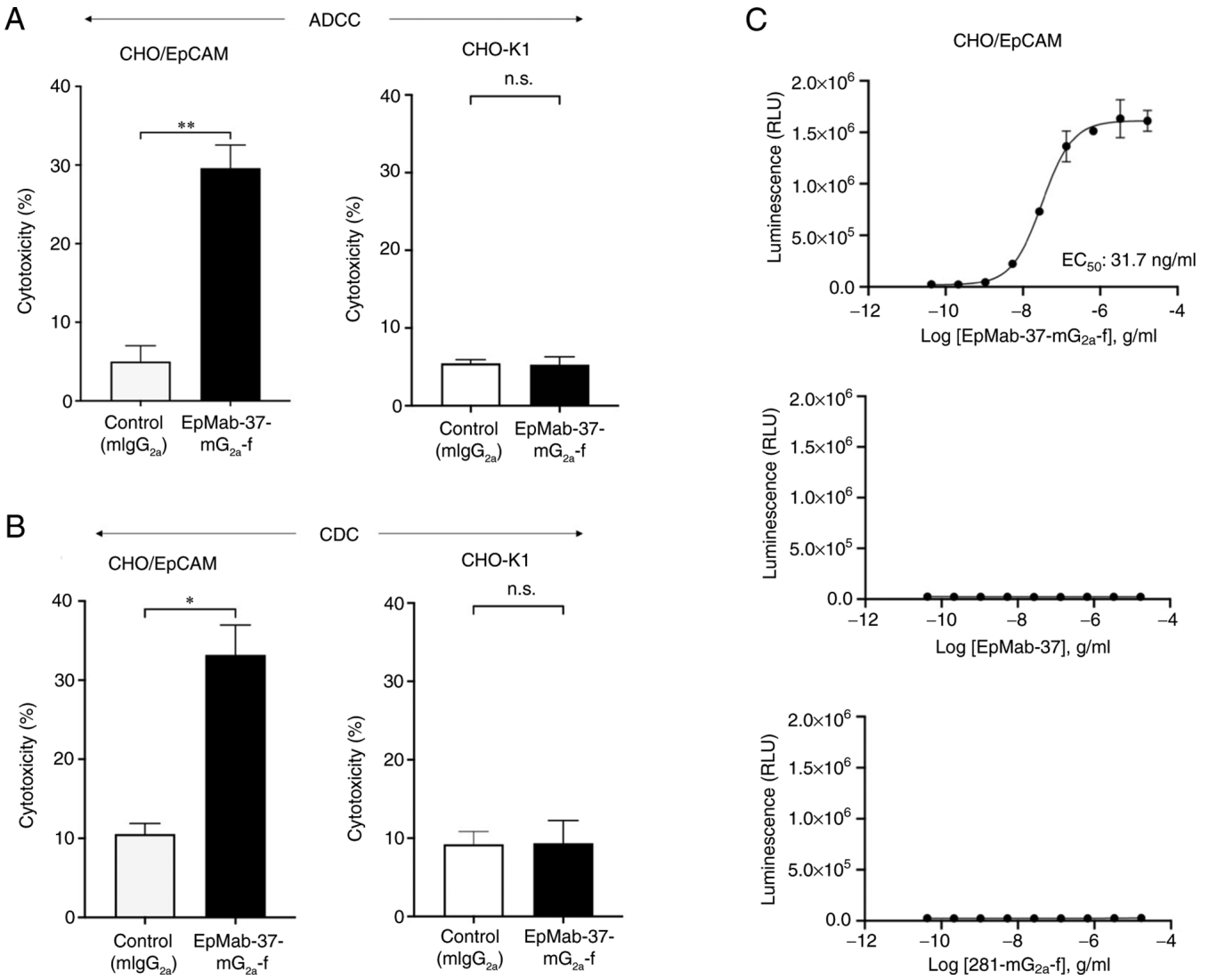

Figure 2. Evaluation of ADCC and CDC elicited by EpMab-37-mG_{2a}-f. (A) ADCC elicited by EpMab-37-mG_{2a}-f and $mIgG_{2a}$ targeting CHO/EpCAM and CHO-K1 cells. (B) CDC elicited by EpMab-37-mG_{2a}-f and control mouse IgG_{2a} targeting CHO/EpCAM and CHO-K1 cells. Values are presented as the mean ± SEM (*P<0.05 and **P<0.01; Welch's t-test). (C) ADCC reporter bioassay by EpMab-37-mG_{2a}-f, EpMab-37, and control (281-mG_{2a}-f) in the presence of CHO/EpCAM cells. ADCC, antibody-dependent cellular cytotoxicity; CDC, complement-dependent cytotoxicity; n.s., not significant; $mIgG_{2a}$, mouse IgG_{2a}; CHO, Chinese hamster ovary; EpCAM, epithelial cell adhesion molecule.

ANOVA with Sidak's post hoc test were utilized for tumor volume and mice weight. GraphPad Prism 8 (GraphPad Software, Inc.) was used for all calculations. P<0.05 was considered to indicate a statistically significant difference.

Results

Flow cytometric analysis against CHO/EpCAM cells using EpMab-37-mG_{2a}-f. In a previous study by the authors, an anti-EpCAM mAb (EpMab-37, mouse IgG_1, kappa) was established, using cancer-specific mAb (CasMab) technology (25). EpMab-37 was revealed to be available for flow cytometry, western blotting and immunohistochemistry (25). In the present study, a defucosylated form of anti-EpCAM mAb (EpMab-37-mG_{2a}-f) was produced by combining V_H and V_L of EpMab-37 with C_H and C_L of mouse IgG_{2a}, respectively (Fig. 1A). EpMab-37-mG_{2a}-f detected CHO/EpCAM and not parental CHO-K1 cells in a concentration-dependent manner (Figs. 1B and S1A), indicating that EpMab-37-mG_{2a}-f reacted with EpCAM.

A kinetic analysis of the interactions of EpMab-37-mG_{2a}-f with CHO/EpCAM was performed using flow cytometry. As demonstrated in Fig. 1C, the K_D for the interaction of EpMab-37-mG_{2a}-f with CHO/EpCAM cells was $2.2x10^{-8}$ M, suggesting that EpMab-37-mG_{2a}-f may exhibit moderate affinity for CHO/EpCAM cells.

EpMab-37-mG_{2a}-f-mediated ADCC and CDC in CHO/EpCAM cells. The present study then investigated whether EpMab-37-mG_{2a}-f was capable of mediating ADCC against CHO/EpCAM cells. EpMab-37-mG_{2a}-f exhibited ADCC (29.6% cytotoxicity) against CHO/EpCAM cells more effectively than the control mouse IgG_{2a} (5.0% cytotoxicity; P<0.01). No notable difference was found between EpMab-37-mG_{2a}-f and control mouse IgG_{2a} in ADCC levels against CHO-K1 (Fig. 2A).

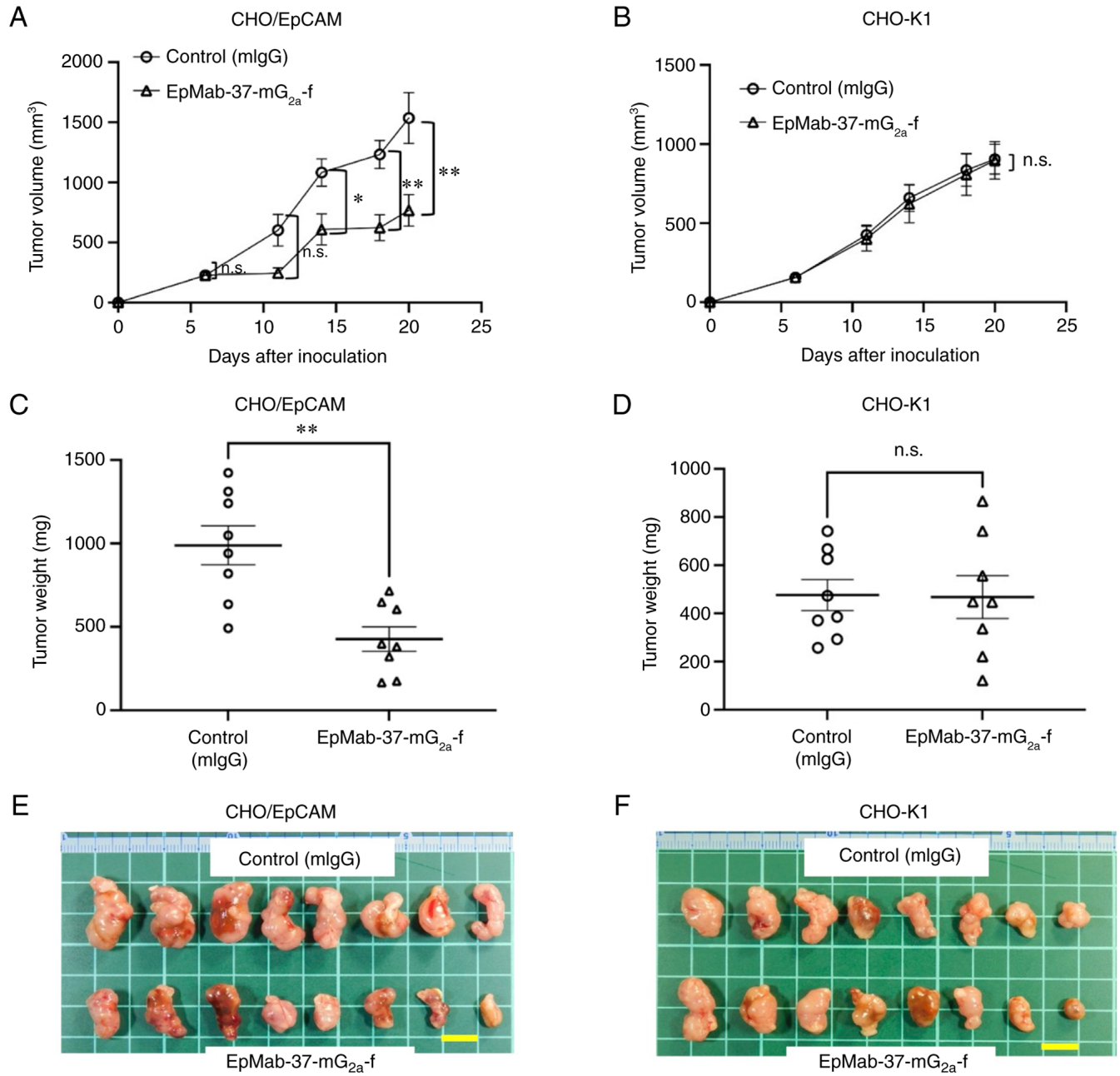

Figure 3. Antitumor activity of EpMab-37-mG$_{2a}$-f. (A and B) Measurement of tumor volume in (A) CHO/EpCAM and (B) CHO-K1 xenograft models. CHO/EpCAM and CHO-K1 cells (5x10^6 cells) were injected into mice subcutaneously. On day 6, 100 μg EpMab-37-mG$_{2a}$-f or mIgG were injected into mice intraperitoneally. On day 14, additional antibodies were injected. On days 6, 11, 14, 18 and 20 following the inoculation, the tumor volume was measured. Values are presented as the mean ± SEM. *P<0.05 and **P<0.01 (ANOVA and Sidak's multiple comparisons test). (C and D) The weight of the excised (C) CHO/EpCAM and (D) CHO-K1 xenografts was measured on day 20. Values are presented as the mean ± SEM. **P<0.01 (Welch's t-test). (E and F) The resected tumors appearance of (E) CHO/EpCAM and (F) CHO-K1 xenografts in the control mouse IgG and EpMab-37-mG$_{2a}$-f treated groups on day 20 (scale bar, 1 cm). n.s., not significant; CHO, Chinese hamster ovary; EpCAM, epithelial cell adhesion molecule; mIgG, mouse IgG.

Subsequently, it was examined whether EpMab-37-mG$_{2a}$-f could exert CDC against CHO/EpCAM cells. As demonstrated in Fig. 2B, EpMab-37-mG$_{2a}$-f induced a higher degree of CDC (33.2% cytotoxicity) in CHO/EpCAM cells compared with that induced by control mouse IgG$_{2a}$ (10.5% cytotoxicity; P<0.05). There was no marked difference between EpMab-37-mG$_{2a}$-f and control mouse IgG$_{2a}$ in the observed CDC levels against CHO-K1 (Fig. 2B).

The ADCC reporter bioassay is a bioluminescent reporter gene assay for the quantification of the biological activity of the antibody via FcγRIIIa-mediated pathway activation in an ADCC mechanism of action (40). In the present study, to compare the ADCC pathway activation by EpMab-37-mG$_{2a}$-f and EpMab-37, the CHO/EpCAM cells were treated with serially diluted mAbs, and then incubated with effector Jurkat cells, which express the human FcγRIIIa receptor and an NFAT response element driving Firefly luciferase. Furthermore, defucosylated anti-hamster PDPN (mouse IgG$_{2a}$ Ab) (281-mG$_{2a}$-f) was also used as a control since defucosylated control mouse IgG$_{2a}$ was unavailable. It was confirmed that 281-mG$_{2a}$-f never recognized the target cells. As demonstrated in Fig. 2C, EpMab-37-mG$_{2a}$-f activated

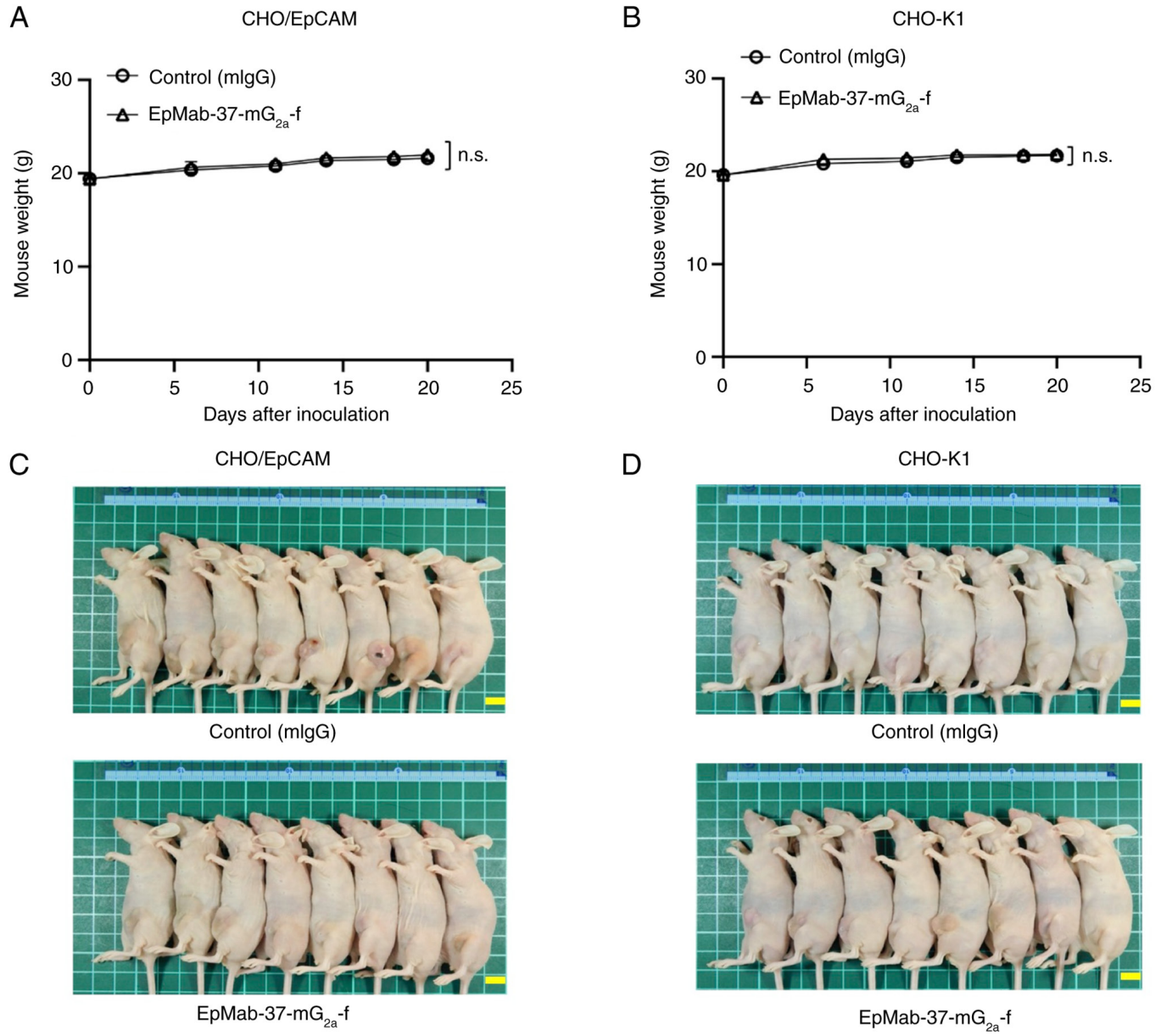

Figure 4. Mouse body weights and appearance. (A and B) Body weights of (A) CHO/EpCAM and (B) CHO-K1 xenografts-implanted mice on days 6, 11, 14, 18 and 20 (ANOVA and Sidak's multiple comparisons test). (C and D) Body appearance of (C) CHO/EpCAM and (D) CHO-K1 xenografts-implanted mice on day 20 (scale bar, 1 cm). n.s., not significant; CHO, Chinese hamster ovary; EpCAM, epithelial cell adhesion molecule; mIgG, mouse IgG.

the effector (EC_{50}; 31.7 ng/ml) in a concentration-dependent manner, whereas EpMab-37 and 281-mG_{2a}-f did not. These results indicated that EpMab-37-mG_{2a}-f exhibits superior ADCC activity against CHO/EpCAM cells compared with EpMab-37.

Antitumor effects of EpMab-37-mG_{2a}-f in the mouse xenografts of CHO/EpCAM cells. In the CHO/EpCAM xenograft tumors, EpMab-37-mG_{2a}-f and control mouse IgG were injected into mice intraperitoneally on days 6 and 14, following CHO/EpCAM cell inoculation. On days 6, 11, 14, 18 and 20 following the inoculation, the tumor volume was measured. The EpMab-37-mG_{2a}-f administration resulted in a significant reduction in tumor volume on days 14 ($P<0.05$), 18 ($P<0.01$) and 20 ($P<0.01$) compared with that of the control mouse IgG (Fig. 3A). The EpMab-37-mG_{2a}-f administration resulted in a 50% reduction in tumor volume compared with that of the control mouse IgG on day 20.

The weight of CHO/EpCAM tumors treated with EpMab-37-mG_{2a}-f was significantly lower than that of tumors treated with control mouse IgG (57% reduction; $P<0.01$; Fig. 3C). CHO/EpCAM tumors that were resected from mice on day 20 are depicted in Fig. 3E.

In the CHO-K1 xenograft models, EpMab-37-mG_{2a}-f and control mouse IgG were intraperitoneally injected into mice on days 6 and 14 following the inoculation of CHO-K1 cells. On days 6, 11, 14, 18 and 20 after the inoculation of cells, the tumor volume was measured. No marked differences were observed between EpMab-37-mG_{2a}-f and control mouse IgG as regards CHO-K1 tumor volume (Fig. 3B) and weight (Fig. 3D). CHO-K1 tumors that were resected from mice on day 20 are demonstrated in Fig. 3F.

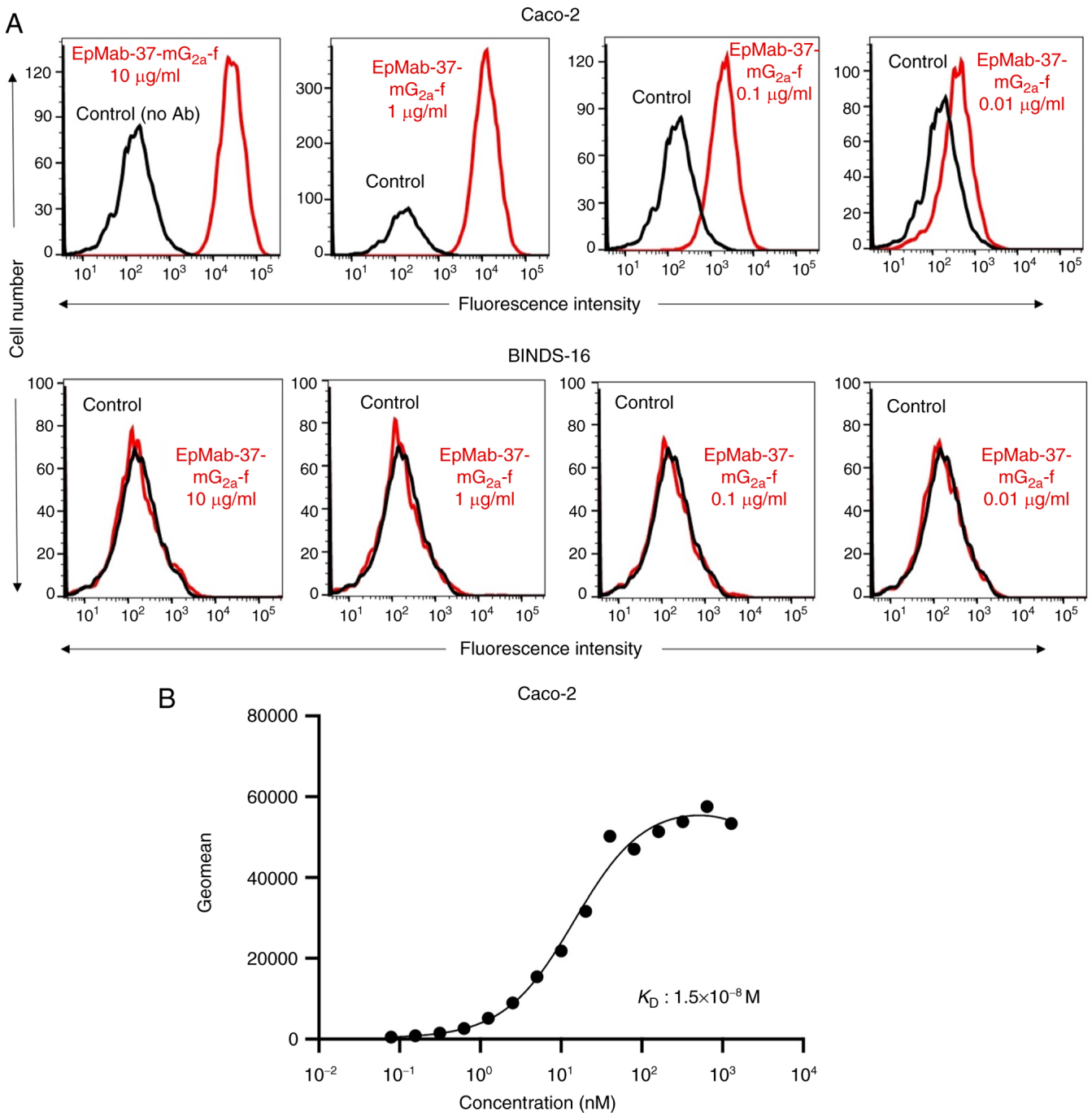

Figure 5. Flow cytometry of EpMab-37-mG$_{2a}$-f against the human colorectal cancer cell line, Caco-2, and Caco-2 cells in which EpCAM was knocked out (BINDS-16). (A) Caco-2 and BINDS-16 cells were treated with EpMab-37-mG$_{2a}$-f (red) or buffer control (black), followed by Alexa Fluor 488-conjugated anti-mouse IgG. Fluorescence data were analyzed using the SA3800 Cell Analyzer. (B) Determination of the binding affinity of EpMab-37-mG$_{2a}$-f for Caco-2 cells using flow cytometry. Caco-2 cells were suspended in 100 μl serially diluted EpMab-37-mG$_{2a}$-f. Alexa Fluor 488-conjugated anti-mouse IgG was then added. Fluorescence data were collected using the BD FACSLyric and the K_D was calculated by GraphPad PRISM 8. EpCAM, epithelial cell adhesion molecule; K_D, dissociation constant.

The loss of body weight was not observed in the CHO/EpCAM (Fig. 4A) and CHO-K1 (Fig. 4B) tumor-implanted mice. The mice on day 20 are demonstrated in Fig. 4C and D.

Flow cytometry of Caco-2 cells using EpMab-37-mG$_{2a}$-f. As demonstrated in Figs. 5A and S1B, EpMab-37-mG$_{2a}$-f detected Caco-2 cells in a concentration-dependent manner. By contrast, EpMab-37 did not react with Caco-2 cells in which EpCAM was knocked out (BINDS-16). The increased expression of EpCAM could also be detected in other colorectal cancer cell lines tested (Fig. S2). A kinetic analysis of the binding of EpMab-37-mG$_{2a}$-f to Caco-2 cells was performed using flow cytometry. The K_D for the interaction of EpMab-37-mG$_{2a}$-f with Caco-2 cells was 1.5x10^{-8} M (Fig. 5B), suggesting that EpMab-37-mG$_{2a}$-f exhibits moderate affinity for Caco-2 cells.

EpMab-37-mG$_{2a}$-f-mediated ADCC and CDC in Caco-2 and BINDS-16 cells. The present study then investigated whether

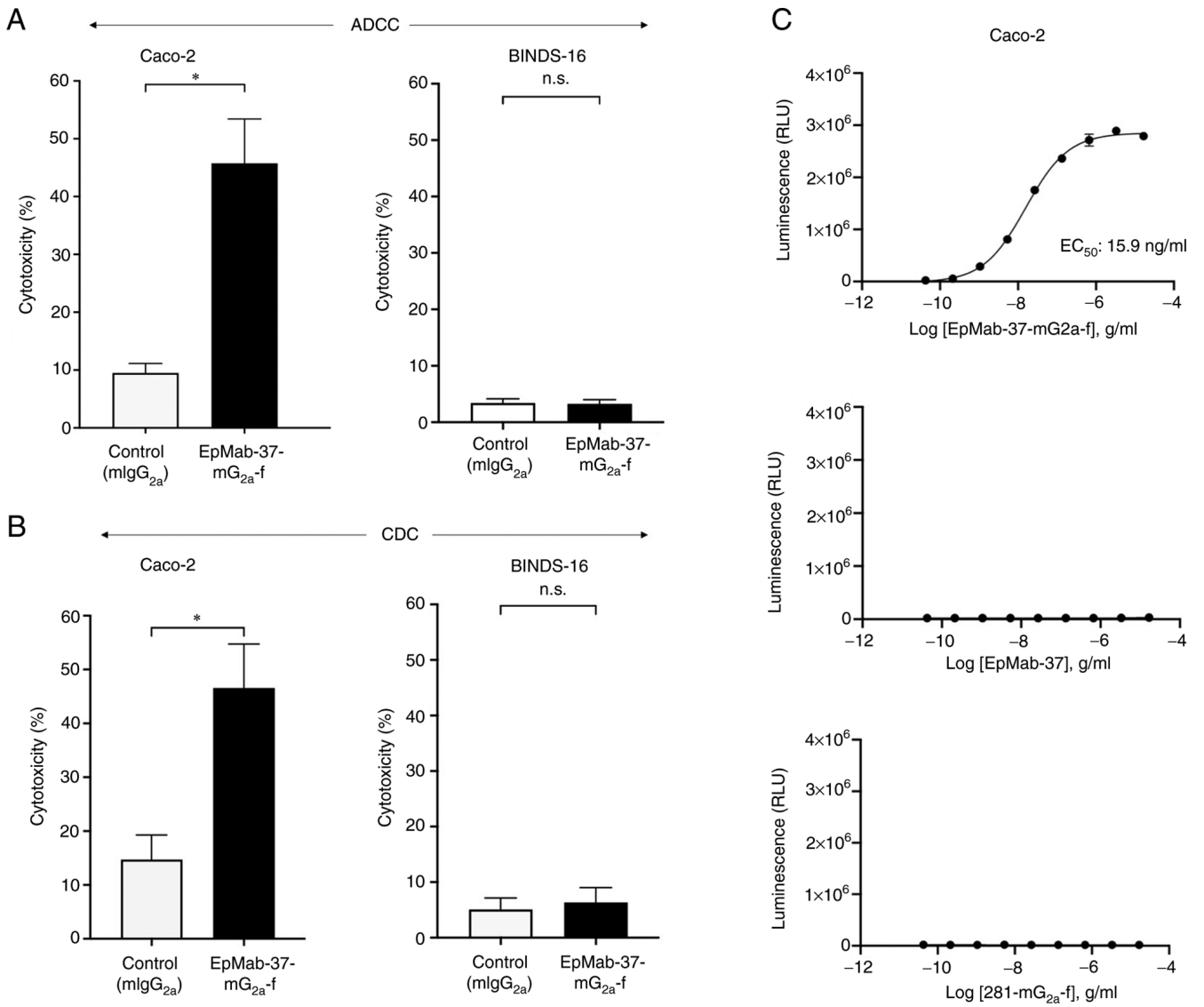

Figure 6. ADCC and CDC activity of EpMab-37-mG_{2a}-f against Caco-2 and BINDS-16 cells (Caco-2 cells in which EpCAM was knocked out). (A) ADCC elicited by EpMab-37-mG_{2a}-f and control mouse IgG_{2a} ($mIgG_{2a}$) targeting Caco-2 and BINDS-16 cells. (B) CDC elicited by EpMab-37-mG_{2a}-f and control mouse IgG_{2a} targeting Caco-2 and BINDS-16 cells. Values are presented as the mean ± SEM. *P<0.05 (Welch's t-test). (C) ADCC reporter bioassay by EpMab-37-mG_{2a}-f, EpMab-37, and control (281-mG_{2a}-f) in the presence of Caco-2 cells. ADCC, antibody-dependent cellular cytotoxicity; CDC, complement-dependent cytotoxicity; n.s., not significant; $mIgG_{2a}$, mouse IgG_{2a}; CHO, Chinese hamster ovary; EpCAM, epithelial cell adhesion molecule.

EpMab-37-mG_{2a}-f is capable of mediating ADCC against Caco-2 and BINDS-16 cells. As revealed in Fig. 6A, EpMab-37-mG_{2a}-f demonstrated ADCC (45.7% cytotoxicity) against Caco-2 cells, more potently than the control mouse IgG_{2a} (9.5% cytotoxicity; P<0.05). It was then investigated whether EpMab-37-mG_{2a}-f exhibited CDC against Caco-2 cells. EpMab-37-mG_{2a}-f induced a higher degree of CDC (46.6% cytotoxicity) in Caco-2 cells compared with that induced by control mouse IgG_{2a} (14.7% cytotoxicity; P<0.05) (Fig. 6B). By contrast, ADCC and CDC were not induced by EpMab-37-mG_{2a}-f in BINDS-16 cells (Fig. 6A and B). The ADCC reporter bioassay for Caco-2 cells also revealed that the only EpMab-37-mG_{2a}-f exhibited the ADCC effector activation (EC_{50}; 15.9 ng/ml) (Fig. 6C). These results demonstrated that EpMab-37-mG_{2a}-f exhibited potent ADCC and CDC against Caco-2 cells.

Antitumor effects of EpMab-37-mG_{2a}-f on Caco-2 and BINDS-16 xenografts. In the Caco-2 xenograft models, EpMab-37-mG_{2a}-f and control mouse IgG were intraperitoneally injected on days 6, 14 and 20, following the inoculation of Caco-2 cells. The tumor volume was measured on days 6, 11, 14, 18, 20, 25 and 27 after the injection. The administration of EpMab-37-mG_{2a}-f resulted in a significant reduction in tumor growth on days 14 (P<0.05), 18 (P<0.01), 20 (P<0.01), 25 (P<0.01) and 27 (P<0.01) as compared with the control mouse IgG (Fig. 7A). The administration of EpMab-37-mG_{2a}-f resulted in a 42% reduction in tumor volume compared with the control mouse IgG on day 27. Tumors from the EpMab-37-mG_{2a}-f-treated mice weighed significantly less than those from the control mouse IgG-treated mice (28% reduction; P<0.01, Fig. 7C). Tumors that were resected from mice on day 27 are demonstrated in Fig. 7E. By contrast, the antitumor effects of EpMab-37-mG_{2a}-f on BINDS-16 were not observed (Fig. 7B and D). BINDS-16 tumors that were resected from mice on day 27 are demonstrated in Fig. 7F.

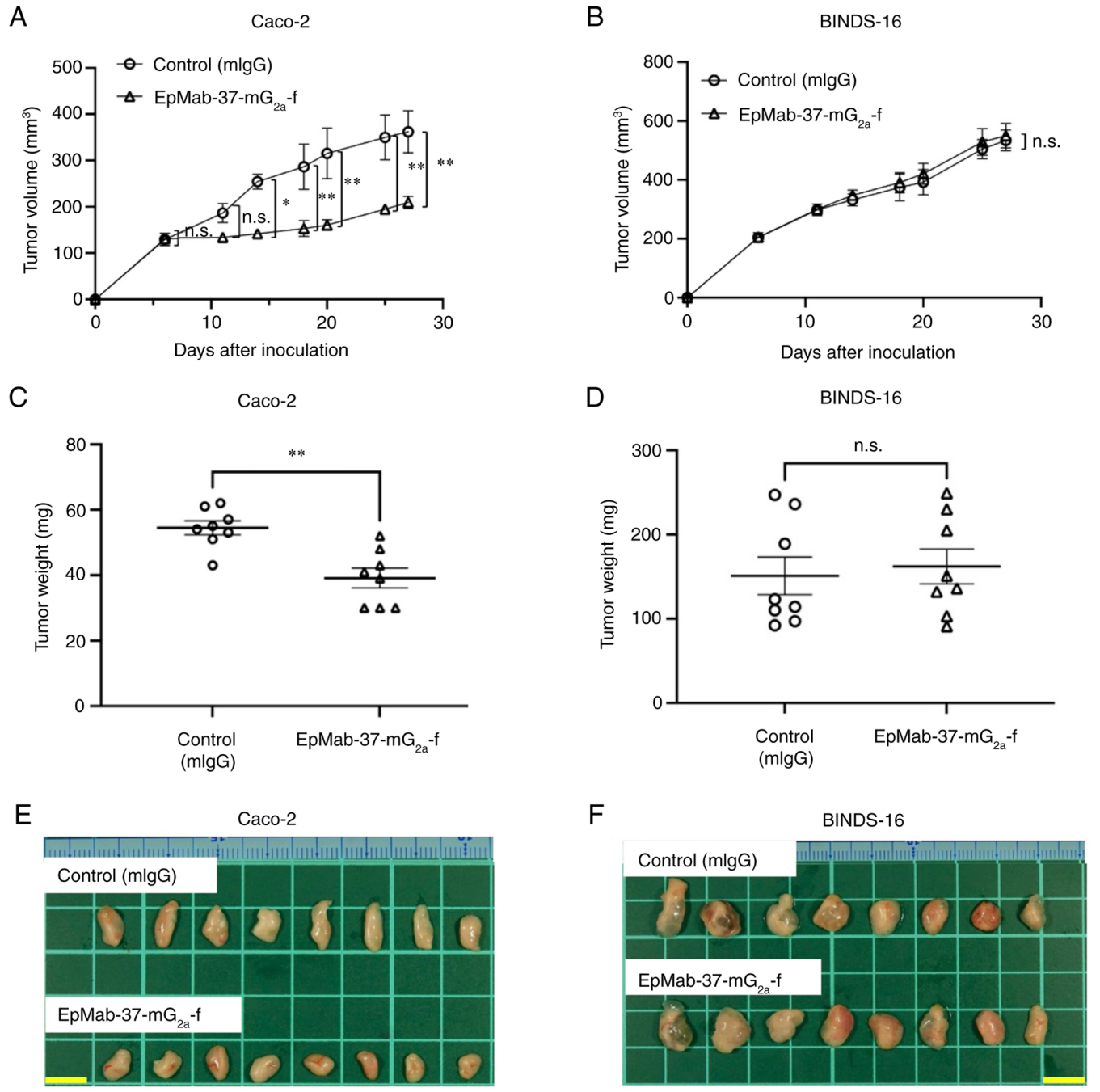

Figure 7. Antitumor activity of EpMab-37-mG$_{2a}$-f against Caco-2 and BINDS-16 xenografts. (A and B) Measurement of tumor volume in (A) Caco-2 and (B) BINDS-16 (Caco-2 cells in which EpCAM was knocked out) xenograft-implanted mice. Caco-2 and BINDS-16 cells (5x10^6 cells) were inoculated into mice subcutaneously. On day 6, 100 μg EpMab-37-mG$_{2a}$-f or mIgG were injected into mice intraperitoneally. On days 14 and 20, additional antibodies were injected. On days 6, 11, 14, 18, 20, 25 and 27 following the inoculation, the tumor volume was measured. Values are presented as the mean ± SEM. *P<0.05 and **P<0.01 (ANOVA and Sidak's multiple comparisons test). (C and D) The weight of excised xenografts of (C) Caco-2 and (D) BINDS-16 was measured on day 27. Values are presented as the mean ± SEM. **P<0.01 (Welch's t-test). (E and F) The resected tumors appearance of (E) Caco-2 and (F) BINDS-16 xenografts in the control mouse IgG and EpMab-37-mG$_{2a}$-f treated groups on day 27 (scale bar, 1 cm). n.s., not significant; mIgG, mouse IgG; EpCAM, epithelial cell adhesion molecule.

The loss of body weight was not observed in Caco-2 and BINDS-16 tumor-implanted mice (Fig. 8A and B). The mice on day 27 are demonstrated in Fig. 8C and D.

Discussion

In the present study, a mouse IgG$_1$ subclass of EpMab-37 was converted into a mouse IgG$_{2a}$, and a defucosylated form (EpMab-37-mG$_{2a}$-f) was produced in order to enhance ADCC activity. In fact, EpMab-37-mG$_{2a}$-f exhibited a high ADCC activity *in vitro* (Figs. 2 and 6), and exhibited potent antitumor activity against CHO/EpCAM (Fig. 3A and C) and Caco-2 xenografts (Fig. 7A and C). Notably, EpMab-37-mG$_{2a}$-f did not affect the growth of tumors derived from Caco-2 cells in which EpCAM was knocked out (BINDS-16) (Fig. 7B and D), indicating that EpMab-37-mG$_{2a}$-f can target EpCAM-positive

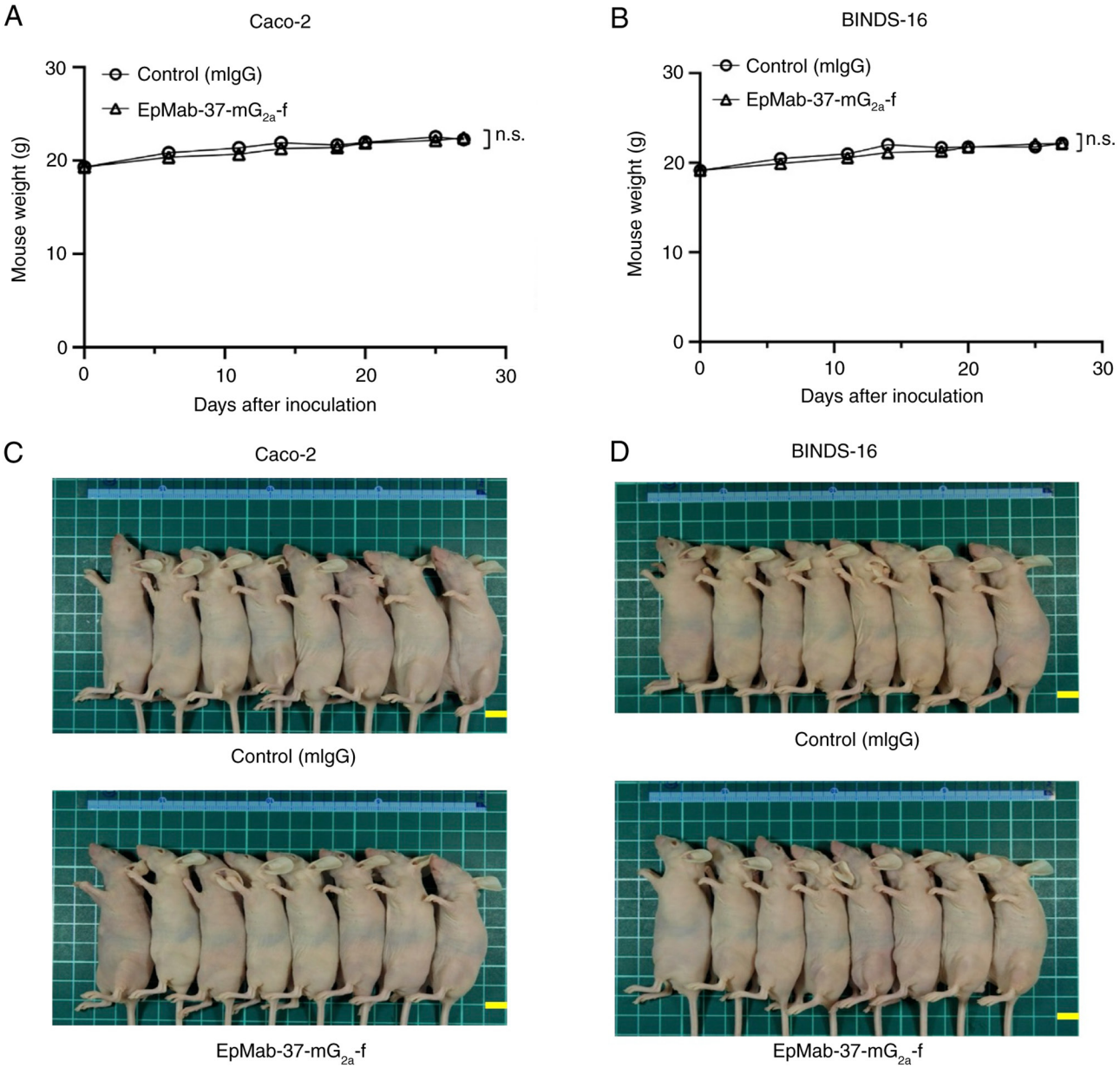

Figure 8. Mouse body weights and appearance. (A and B) Body weights of (A) Caco-2 and (B) BINDS-16 xenografts-implanted mice on days 6, 11, 14, 18, 20, 25 and 27 (ANOVA and Sidak's multiple comparisons test). (C and D) Body appearance of (C) Caco-2 and (D) BINDS-16-xenografts-implanted mice on day 27 (scale bar, 1 cm). n.s., not significant.

tumors selectively. Additionally, it was observed that a higher EpCAM expression could be detected in HCT-15, COLO201 and COLO205 than Caco-2 cells (Fig. S2). Further studies are required to investigate the antitumor activity of EpMab-37-mG_{2a}-f against these cell lines.

The EpCAM N-terminal domain (residues 24-63) contains the EGF-like domain, which is targeted by the vast majority of anti-EpCAM mAbs, including HEA125 (used in CellSearch®), 17-1A (Edrecolomab), C215 (used in Catumaxomab) and MOC31 (used in Oportuzumab) probably due to its high accessibility and antigenicity on plasma membrane (43,44). By contrast, the anti-EpCAM mAbs targeting the thyroglobulin-like domain (residues 64-138) or the extracellular C-terminal domain (residues 139-265; CD) are rare (43). Among the clinically tested mAbs, MT201 (Adecatumumab) was reported to recognize the $_{167}$-QKEIT-$_{171}$ sequence in the EpCAM CD (45). The epitope mapping of EpMab-37 was previously performed by the authors and revealed that EpCAM (residues 144-164) are involved in its recognition (25). In crystal structure analysis, this domain forms β-sheet and loop structures, and exposed on the molecular surface when EpCAM forms cis-dimer or trans-tetramer (43). Therefore, EpMab-37 has a unique epitope, and is expected a different mode of action. However, EpMab-37 never recognized EpCAM peptides including 144 to 163 amino acids, suggesting that EpMab-37 has the conformational epitopes (25). To determine the conformational epitopes, the epitope mapping strategy was developed, including Arg, Ile, Glu, Asp and Leu (RIEDL)-insertion for epitope mapping (REMAP) (46-49) and His-tag insertion for the epitope mapping (HisMAP) method (50,51). The detailed determination of EpMab-37 epitope could contribute the understanding of recognition by EpMab-37.

It was observed that tumors derived from Caco-2 cells in which EpCAM was knocked out exhibited a larger weight and volume compared to parental ones (Fig. 7). Huang *et al* (52) reviewed the effect of EpCAM depletion in Caco-2 cells and *Xenopus* embryos. In EpCAM-depleted Caco-2 cells, the elevated PKC activity resulted in the downregulation of E-cadherin. A similar phenomenon was observed in *Xenopus* embryos (53). Huang *et al* (52) mentioned that these events were 'two noteworthy exceptions' in the regulation of Cadherins by EpCAM. E-cadherin downregulation sometimes leads to epithelial-to-mesenchymal transition and an increase in tumorigenicity (54). Although the *in vitro* cell proliferation of parental and EpCAM knocked out Caco-2 is similar in the experiments of the present study, the aforementioned phenomenon may influence the growth *in vivo*.

In the present study, mouse IgG_{2a} and 281-mG_{2a}-f were used as controls in ADCC/CDC and ADCC reporter assays, respectively, which are mAbs that could recognize unknown (mouse IgG_{2a}) and known (281-mG_{2a}-f) targets. It was confirmed that they were not specific for the target cells. Therefore, they are suitable as negative controls *in vitro* for ADCC/CDC and ADCC reporter assays. However, concerning the *in vivo* analysis, it could not be excluded that they recognize unidentified target and exhibit the side effects in mice. For the aforementioned reasons, normal mouse IgG (a mixture of diverse antibodies) was used as the control in the xenograft assays. In future xenograft studies, it will be also necessary to test IgG, IgG_{2a} and/or 281-mG_{2a}-f and EpMab-37-mG_{2a}-f.

EpCAM-overexpressing CTCs exhibit cancer stem cell features (55). CTCs, which express EpCAM, CD44, CD47 and MET, identify as a subset with increased metastasis-initiating phenotype (56), suggesting that EpCAM plays a crucial role in cancer stemness and metastasis. Recently, CTC expansion methods, including two-dimensional (2D) long-term expansion, 3D organoids/spheroids culture, and xenografts, have been developed to evaluate the character of CTCs (57). Therefore, the biological characteristic of affecting cell proliferation and invasion need to be investigated as Adecatumumab, which has an epitope close to that of EpMab-37, exerts weak anti-proliferative effects in the absence of complement and immune effector cells (45). Moreover, it would be worthwhile to investigate the effect of EpMab-37-mG_{2a}-f on the CTC expansion *in vitro* and metastasis *in vivo*.

Antibody-drug conjugate (ADC) exhibits cytotoxicity through the contents released from endocytic receptor-bound mAbs-drug conjugate (9). Oportuzumab monatox (Vicinium, VB4-845) is an EpCAM-targeting scFv, conjugated with *Pseudomonas* exotoxin A, an inhibitor of translation through ADP-ribosylation of eukaryotic elongation factor-2 (58). Vicinium has been developed for the treatment of bacillus Calmette-Guérin (BCG)-unresponsive non-muscle invasive bladder cancer (NMIBC) (15). Vicinium was approved by the FDA as fast track designation and evaluated in the single-arm Phase 3 VISTA study (NCT02449239) for the patients with high-grade NMIBC previously treated with BCG. However, FDA did not approve Vicinium for BCG-unresponsive NMIBC (59). An anti-dog PDPN mAb conjugated antibody with emtansine was developed as the contents (P38B-DM1) (60-62) P38B-DM1 exhibited cytotoxicity to dog PDPN expressed CHO-K1 cells, and demonstrated more a potent anti-tumor effect than P38B in the xenograft model (63). Moreover, anti-trophoblast cell-surface antigen 2 (TROP2) ADC (Sacituzumab govitecan-hziy) has been approved by the FDA (64). TROP2 is a paralogue of EpCAM (65). As Sacituzumab possesses the potent internalization activity of TROP2 (66), the capacity of EpCAM internalization by EpMab-37-mG_{2a}-f needs to be further investigated for the development of the ADC.

The applications of anti-EpCAM mAbs in the clinic are still limited, since anti-EpCAM mAbs may generate side-effects by affecting normal tissues. CasMabs targeting PDPN (67-70) and podocalyxin (71) have been previously developed by the authors, which are currently applied to chimeric antigen receptor T-cell therapy in mice models (72-74). It will be of great value to establish cancer-specific anti-EpCAM mAbs using the CasMab method. In the future, anti-EpCAM CasMab production may be applicable as a basis for designing and optimizing potent immunotherapy modalities, including ADCs and chimeric antigen receptor T-cell therapy.

Acknowledgements

The authors would like to thank Ms. Saori Okuno and Ms. Saori Handa (Department of Antibody Drug Development, Tohoku University Graduate School of Medicine) for providing technical assistance for the completion of the *in vitro* experiments, and Mr. Shun-ichi Ohba and Ms. Akiko Harakawa [Institute of Microbial Chemistry (BIKAKEN), Numazu, Microbial Chemistry Research Foundation] for providing technical assistance in performing the animal experiments.

Funding

The present study was supported in part by Japan Agency for Medical Research and Development (AMED; grant nos. JP22ama121008, JP21am0401013, JP22bm1004001, JP22ck0106730 and JP21am0101078).

Availability of data and materials

The datasets used and/or analyzed during the current study are available from the corresponding author on reasonable request.

Authors' contributions

GL, TO, TT, MY, TN, TA and TY performed the experiments. MKK, MK and YK designed the experiments. GL, TO, HS and YK analyzed the data. GL, HS, and YK wrote the manuscript. All authors have read and approved the final manuscript and agree to be accountable for all aspects of the research in ensuring that the accuracy or integrity of any part of the work are appropriately investigated and resolved. HS and YK confirm the authenticity of all the raw data.

Ethics approval and consent to participate

The animal study protocol was approved (approval no. 2022-024) by the Institutional Committee for Experiments of the Institute of Microbial Chemistry (Numazu, Japan).

Patient consent for publication

Not applicable.

Competing interests

The authors declare that they have no competing interests.

References

1. Trzpis M, McLaughlin PM, de Leij LM and Harmsen MC: Epithelial cell adhesion molecule: More than a carcinoma marker and adhesion molecule. Am J Pathol 171: 386-395, 2007.
2. Brown TC, Sankpal NV and Gillanders WE: Functional implications of the dynamic regulation of EpCAM during epithelial-to-mesenchymal transition. Biomolecules 11: 956, 2021.
3. Eyvazi S, Farajnia S, Dastmalchi S, Kanipour F, Zarredar H and Bandehpour M: Antibody based EpCAM targeted therapy of cancer, review and update. Curr Cancer Drug Targets 18: 857-868, 2018.
4. Xiao J, Pohlmann PR, Isaacs C, Weinberg BA, He AR, Schlegel R and Agarwal S: Circulating tumor cells: Technologies and their clinical potential in cancer metastasis. Biomedicines 9: 1111, 2021.
5. de Bono JS, Scher HI, Montgomery RB, Parker C, Miller MC, Tissing H, Doyle GV, Terstappen LW, Pienta KJ and Raghavan D: Circulating tumor cells predict survival benefit from treatment in metastatic castration-resistant prostate cancer. Clin Cancer Res 14: 6302-6309, 2008.
6. Watanabe M, Kenmotsu H, Ko R, Wakuda K, Ono A, Imai H, Taira T, Naito T, Murakami H, Abe M, *et al*: Isolation and molecular analysis of circulating tumor cells from lung cancer patients using a microfluidic chip type cell sorter. Cancer Sci 109: 2539-2548, 2018.
7. Lampignano R, Yang L, Neumann MHD, Franken A, Fehm T, Niederacher D and Neubauer H: A novel workflow to enrich and isolate patient-matched EpCAMhigh and EpCAM$^{low/negative}$ CTCs enables the comparative characterization of the PIK3CA status in metastatic breast cancer. Int J Mol Sci 18: 1885, 2017.
8. Zapatero A, Gómez-Caamaño A, Cabeza Rodriguez MÁ, Muinelo-Romay L, Martin de Vidales C, Abalo A, Calvo Crespo P, Leon Mateos L, Olivier C and Vega Piris LV: Detection and dynamics of circulating tumor cells in patients with high-risk prostate cancer treated with radiotherapy and hormones: A prospective phase II study. Radiat Oncol 15: 137, 2020.
9. Tsao LC, Force J and Hartman ZC: Mechanisms of therapeutic antitumor monoclonal antibodies. Cancer Res 81: 4641-4651, 2021.
10. McInnes IB and Gravallese EM: Immune-mediated inflammatory disease therapeutics: Past, present and future. Nat Rev Immunol 21: 680-686, 2021.
11. Herlyn M, Steplewski Z, Herlyn D and Koprowski H: Colorectal carcinoma-specific antigen: Detection by means of monoclonal antibodies. Proc Natl Acad Sci USA 76: 1438-1442, 1979.
12. Baeuerle PA and Gires O: EpCAM (CD326) finding its role in cancer. Br J Cancer 96: 417-423, 2007.
13. Sears HF, Atkinson B, Mattis J, Ernst C, Herlyn D, Steplewski Z, Häyry P and Koprowski H: Phase-I clinical trial of monoclonal antibody in treatment of gastrointestinal tumours. Lancet 1: 762-765, 1982.
14. Riethmüller G, Holz E, Schlimok G, Schmiegel W, Raab R, Höffken K, Gruber R, Funke I, Pichlmaier H, Hirche H, *et al*: Monoclonal antibody therapy for resected Dukes' C colorectal cancer: Seven-year outcome of a multicenter randomized trial. J Clin Oncol 16: 1788-1794, 1998.
15. Kaplon H, Muralidharan M, Schneider Z and Reichert JM: Antibodies to watch in 2020. MAbs 12: 1703531, 2020.
16. Zhang X, Yang Y, Fan D and Xiong D: The development of bispecific antibodies and their applications in tumor immune escape. Exp Hematol Oncol 6: 12, 2017.
17. Schönberger S, Kraft D, Nettersheim D, Schorle H, Casati A, Craveiro RB, Mohseni MM, Calaminus G and Dilloo D: Targeting EpCAM by a bispecific trifunctional antibody exerts profound cytotoxic efficacy in germ cell tumor cell lines. Cancers (Basel) 12: 1279, 2020.
18. Ruf P, Kluge M, Jäger M, Burges A, Volovat C, Heiss MM, Hess J, Wimberger P, Brandt B and Lindhofer H: Pharmacokinetics, immunogenicity and bioactivity of the therapeutic antibody catumaxomab intraperitoneally administered to cancer patients. Br J Clin Pharmacol 69: 617-625, 2010.
19. Mau-Sørensen M, Dittrich C, Dienstmann R, Lassen U, Büchler W, Martinius H and Tabernero J: A phase I trial of intravenous catumaxomab: A bispecific monoclonal antibody targeting EpCAM and the T cell coreceptor CD3. Cancer Chemother Pharmacol 75: 1065-1073, 2015.
20. Knödler M, Körfer J, Kunzmann V, Trojan J, Daum S, Schenk M, Kullmann F, Schroll S, Behringer D, Stahl M, *et al*: Randomised phase II trial to investigate catumaxomab (anti-EpCAM x anti-CD3) for treatment of peritoneal carcinomatosis in patients with gastric cancer. Br J Cancer 119: 296-302, 2018.
21. Linke R, Klein A and Seimetz D: Catumaxomab: Clinical development and future directions. MAbs 2: 129-136, 2010.
22. Pereira NA, Chan KF, Lin PC and Song Z: The 'less-is-more' in therapeutic antibodies: Afucosylated anti-cancer antibodies with enhanced antibody-dependent cellular cytotoxicity. MAbs 10: 693-711, 2018.
23. Shinkawa T, Nakamura K, Yamane N, Shoji-Hosaka E, Kanda Y, Sakurada M, Uchida K, Anazawa H, Satoh M, Yamasaki M, *et al*: The absence of fucose but not the presence of galactose or bisecting N-acetylglucosamine of human IgG1 complex-type oligosaccharides shows the critical role of enhancing antibody-dependent cellular cytotoxicity. J Biol Chem 278: 3466-3473, 2003.
24. Yamane-Ohnuki N, Kinoshita S, Inoue-Urakubo M, Kusunoki M, Iida S, Nakano R, Wakitani M, Niwa R, Sakurada M, Uchida K, *et al*: Establishment of FUT8 knockout Chinese hamster ovary cells: An ideal host cell line for producing completely defucosylated antibodies with enhanced antibody-dependent cellular cytotoxicity. Biotechnol Bioeng 87: 614-622, 2004.
25. Li G, Suzuki H, Asano T, Tanaka T, Suzuki H, Kaneko MK and Kato Y: Development of a novel anti-EpCAM monoclonal antibody for various applications. Antibodies (Basel) 11: 41, 2022.
26. Hosono H, Ohishi T, Takei J, Asano T, Sayama Y, Kawada M, Kaneko MK and Kato Y: The anti-epithelial cell adhesion molecule (EpCAM) monoclonal antibody EpMab-16 exerts antitumor activity in a mouse model of colorectal adenocarcinoma. Oncol Lett 20: 383, 2020.
27. Kaneko MK, Ohishi T, Takei J, Sano M, Nakamura T, Hosono H, Yanaka M, Asano T, Sayama Y, Harada H, *et al*: Anti-EpCAM monoclonal antibody exerts antitumor activity against oral squamous cell carcinomas. Oncol Rep 44: 2517-2526, 2020.
28. Queiroz AL, Dantas E, Ramsamooj S, Murthy A, Ahmed M, Zunica ERM, Liang RJ, Murphy J, Holman CD, Bare CJ, *et al*: Blocking ActRIIB and restoring appetite reverses cachexia and improves survival in mice with lung cancer. Nat Commun 13: 4633, 2022.
29. Takei J, Kaneko MK, Ohishi T, Hosono H, Nakamura T, Yanaka M, Sano M, Asano T, Sayama Y, Kawada M, *et al*: A defucosylated anti-CD44 monoclonal antibody 5-mG2a-f exerts antitumor effects in mouse xenograft models of oral squamous cell carcinoma. Oncol Rep 44: 1949-1960, 2020.
30. Takei J, Ohishi T, Kaneko MK, Harada H, Kawada M and Kato Y: A defucosylated anti-PD-L1 monoclonal antibody 13-mG_{2a}-f exerts antitumor effects in mouse xenograft models of oral squamous cell carcinoma. Biochem Biophys Rep 24: 100801, 2020.
31. Li G, Ohishi T, Kaneko MK, Takei J, Mizuno T, Kawada M, Saito M, Suzuki H and Kato Y: Defucosylated mouse-dog chimeric anti-EGFR antibody exerts antitumor activities in mouse xenograft models of canine tumors. Cells 10: 3599, 2021.
32. Tateyama N, Nanamiya R, Ohishi T, Takei J, Nakamura T, Yanaka M, Hosono H, Saito M, Asano T, Tanaka T, *et al*: Defucosylated anti-epidermal growth factor receptor monoclonal antibody 134-mG_{2a}-f exerts antitumor activities in mouse xenograft models of dog epidermal growth factor receptor-overexpressed cells. Monoclon Antib Immunodiagn Immunother 40: 177-183, 2021.
33. Goto N, Suzuki H, Ohishi T, Harakawa A, Li G, Saito M, Takei J, Tanaka T, Asano T, Sano M, *et al*: Antitumor activities in mouse xenograft models of canine fibroblastic tumor by defucosylated anti-epidermal growth factor receptor monoclonal antibody. Monoclon Antib Immunodiagn Immunother 41: 67-73, 2022.
34. Nanamiya R, Takei J, Ohishi T, Asano T, Tanaka T, Sano M, Nakamura T, Yanaka M, Handa S, Tateyama N, *et al*: Defucosylated anti-epidermal growth factor receptor monoclonal antibody (134-mG_{2a}-f) exerts antitumor activities in mouse xenograft models of canine osteosarcoma. Monoclon Antib Immunodiagn Immunother 41: 1-7, 2022.
35. Suzuki H, Ohishi T, Asano T, Tanaka T, Saito M, Mizuno T, Yoshikawa T, Kawada M, Kaneko MK and Kato Y: Defucosylated mouse-dog chimeric anti-HER2 monoclonal antibody exerts antitumor activities in mouse xenograft models of canine tumors. Oncol Rep 48: 154, 2022.

36. Tanaka T, Ohishi T, Saito M, Suzuki H, Kaneko MK, Kawada M and Kato Y: Defucosylated anti-epidermal growth factor receptor monoclonal antibody exerted antitumor activities in mouse xenograft models of canine mammary gland tumor. Monoclon Antib Immunodiagn Immunother 41: 142-149, 2022.
37. Nanamiya R, Suzuki H, Takei J, Li G, Goto N, Harada H, Saito M, Tanaka T, Asano T, Kaneko MK and Kato Y: Development of monoclonal antibody 281-mG_{2a}-f against golden hamster podoplanin. Monoclon Antib Immunodiagn Immunother: Apr 27, 2022 (Epub ahead of print).
38. Itai S, Ohishi T, Kaneko MK, Yamada S, Abe S, Nakamura T, Yanaka M, Chang YW, Ohba SI, Nishioka Y, *et al*: Anti-podocalyxin antibody exerts antitumor effects via antibody-dependent cellular cytotoxicity in mouse xenograft models of oral squamous cell carcinoma. Oncotarget 9: 22480-22497, 2018.
39. Takei J, Kaneko MK, Ohishi T, Kawada M, Harada H and Kato Y: A novel anti-EGFR monoclonal antibody (EMab-17) exerts antitumor activity against oral squamous cell carcinomas via antibody-dependent cellular cytotoxicity and complement-dependent cytotoxicity. Oncol Lett 19: 2809-2816, 2020.
40. Garvin D, Stecha P, Gilden J, Wang J, Grailer J, Hartnett J, Fan F, Cong M and Cheng ZJ: Determining ADCC activity of antibody-based therapeutic molecules using two bioluminescent reporter-based bioassays. Curr Protoc 1: e296, 2021.
41. Kosterink JGW, McLaughlin PM, Lub-de Hooge MN, Hendrikse HH, van Zanten J, van Garderen E, Harmsen MC and de Leij LFMH: Biodistribution studies of epithelial cell adhesion molecule (EpCAM)-directed monoclonal antibodies in the EpCAM-transgenic mouse tumor model. J Immunol 179: 1362-1368, 2007.
42. Kato Y, Ohishi T, Takei J, Nakamura T, Kawada M and Kaneko MK: An antihuman epidermal growth factor receptor 2 monoclonal antibody (H_2Mab-19) exerts antitumor activity in glioblastoma xenograft models. Monoclon Antib Immunodiagn Immunother 39: 135-139, 2020.
43. Pavšič M, Gunčar G, Djinović-Carugo K and Lenarčič B: Crystal structure and its bearing towards an understanding of key biological functions of EpCAM. Nat Commun 5: 4764, 2014.
44. Gaber A, Lenarčič B and Pavšič M: Current view on EpCAM structural biology. Cells 9: 1361, 2020.
45. Münz M, Murr A, Kvesic M, Rau D, Mangold S, Pflanz S, Lumsden J, Volkland J, Fagerberg J, Riethmüller G, *et al*: Side-by-side analysis of five clinically tested anti-EpCAM monoclonal antibodies. Cancer Cell Int 10: 44, 2010.
46. Asano T, Kaneko MK and Kato Y: Development of a novel epitope mapping system: RIEDL insertion for epitope mapping method. Monoclon Antib Immunodiagn Immunother 40: 162-167, 2021.
47. Asano T, Kaneko MK, Takei J, Tateyama N and Kato Y: Epitope mapping of the anti-CD44 monoclonal antibody (C_{44}Mab-46) using the REMAP method. Monoclon Antib Immunodiagn Immunother 40: 156-161, 2021.
48. Nanamiya R, Sano M, Asano T, Yanaka M, Nakamura T, Saito M, Tanaka T, Hosono H, Tateyama N, Kaneko MK and Kato Y: Epitope mapping of an anti-human epidermal growth factor receptor monoclonal antibody (EMab-51) using the RIEDL insertion for epitope mapping method. Monoclon Antib Immunodiagn Immunother 40: 149-155, 2021.
49. Sano M, Kaneko MK, Aasano T and Kato Y: Epitope mapping of an antihuman EGFR monoclonal antibody (EMab-134) using the REMAP method. Monoclon Antib Immunodiagn Immunother 40: 191-195, 2021.
50. Asano T, Suzuki H, Kaneko MK and Kato Y: Epitope mapping of rituximab using HisMAP method. Monoclon Antib Immunodiagn Immunother 41: 8-14, 2022.
51. Suzuki H, Asano T, Tanaka T, Kaneko MK and Kato Y: Epitope mapping of the anti-CD20 monoclonal antibodies (C20Mab-11 and 2H7) using HisMAP method. Monoclon Antib Immunodiagn Immunother 41: 20-26, 2022.
52. Huang L, Yang Y, Yang F, Liu S, Zhu Z, Lei Z and Guo J: Functions of EpCAM in physiological processes and diseases (review). Int J Mol Med 42: 1771-1785, 2018.
53. Maghzal N, Kayali HA, Rohani N, Kajava AV and Fagotto F: EpCAM controls actomyosin contractility and cell adhesion by direct inhibition of PKC. Dev Cell 27: 263-277, 2013.
54. Yang J, Antin P, Berx G, Blanpain C, Brabletz T, Bronner M, Campbell K, Cano A, Casanova J, Christofori G, *et al*: Guidelines and definitions for research on epithelial-mesenchymal transition. Nat Rev Mol Cell Biol 21: 341-352, 2020.
55. Munz M, Baeuerle PA and Gires O: The emerging role of EpCAM in cancer and stem cell signaling. Cancer Res 69: 5627-5629, 2009.
56. Baccelli I, Schneeweiss A, Riethdorf S, Stenzinger A, Schillert A, Vogel V, Klein C, Saini M, Bäuerle T, Wallwiener M, *et al*: Identification of a population of blood circulating tumor cells from breast cancer patients that initiates metastasis in a xenograft assay. Nat Biotechnol 31: 539-544, 2013.
57. Rupp B, Ball H, Wuchu F, Nagrath D and Nagrath S: Circulating tumor cells in precision medicine: Challenges and opportunities. Trends Pharmacol Sci 43: 378-391, 2022.
58. Dieffenbach M and Pastan I: Mechanisms of resistance to immunotoxins containing *Pseudomonas* exotoxin A in cancer therapy. Biomolecules 10: 979, 2020.
59. Fragkoulis C, Glykas I, Bamias A, Stathouros G, Papadopoulos G and Ntoumas K: Novel treatments in BCG failure. Where do we stand today? Arch Esp Urol 74: 681-691, 2021 (In English, Spanish).
60. Kaneko MK, Honma R, Ogasawara S, Fujii Y, Nakamura T, Saidoh N, Takagi M, Kagawa Y, Konnai S and Kato Y: PMab-38 recognizes canine podoplanin of squamous cell carcinomas. Monoclon Antib Immunodiagn Immunother 35: 263-266, 2016.
61. Ito A, Ohta M, Kato Y, Inada S, Kato T, Nakata S, Yatabe Y, Goto M, Kaneda N, Kurita K, *et al*: A real-time near-infrared fluorescence imaging method for the detection of oral cancers in mice using an indocyanine green-labeled podoplanin antibody. Technol Cancer Res Treat 17: 1533033818767936, 2018.
62. Kato Y, Ohishi T, Kawada M, Maekawa N, Konnai S, Itai S, Yamada S and Kaneko MK: The mouse-canine chimeric anti-dog podoplanin antibody P38B exerts antitumor activity in mouse xenograft models. Biochem Biophys Rep 17: 23-26, 2018.
63. Kato Y, Ito Y, Ohishi T, Kawada M, Nakamura T, Sayama Y, Sano M, Asano T, Yanaka M, Okamoto S, *et al*: Antibody-drug conjugates using mouse-canine chimeric anti-dog podoplanin antibody exerts antitumor activity in a mouse xenograft model. Monoclon Antib Immunodiagn Immunother 39: 37-44, 2020.
64. Bardia A, Mayer IA, Vahdat LT, Tolaney SM, Isakoff SJ, Diamond JR, O'Shaughnessy J, Moroose RL, Santin AD, Abramson VG, *et al*: Sacituzumab govitecan-hziy in refractory metastatic triple-negative breast cancer. N Engl J Med 380: 741-751, 2019.
65. Pavšič M: Trop2 forms a stable dimer with significant structural differences within the membrane-distal region as compared to EpCAM. Int J Mol Sci 22: 10640, 2021.
66. Cardillo TM, Govindan SV, Sharkey RM, Trisal P and Goldenberg DM: Humanized anti-Trop-2 IgG-SN-38 conjugate for effective treatment of diverse epithelial cancers: Preclinical studies in human cancer xenograft models and monkeys. Clin Cancer Res 17: 3157-3169, 2011.
67. Kato Y and Kaneko MK: A cancer-specific monoclonal antibody recognizes the aberrantly glycosylated podoplanin. Sci Rep 4: 5924, 2014.
68. Kaneko MK, Nakamura T, Kunita A, Fukayama M, Abe S, Nishioka Y, Yamada S, Yanaka M, Saidoh N, Yoshida K, *et al*: ChLpMab-23: Cancer-specific human-mouse chimeric anti-podoplanin antibody exhibits antitumor activity via antibody-dependent cellular cytotoxicity. Monoclon Antib Immunodiagn Immunother 36: 104-112, 2017.
69. Kaneko MK, Yamada S, Nakamura T, Abe S, Nishioka Y, Kunita A, Fukayama M, Fujii Y, Ogasawara S and Kato Y: Antitumor activity of chLpMab-2, a human-mouse chimeric cancer-specific antihuman podoplanin antibody, via antibody-dependent cellular cytotoxicity. Cancer Med 6: 768-777, 2017.
70. Suzuki H, Kaneko MK and Kato Y: Roles of podoplanin in malignant progression of tumor. Cells 11: 575, 2022.
71. Kaneko MK, Ohishi T, Kawada M and Kato Y: A cancer-specific anti-podocalyxin monoclonal antibody (60-mG_{2a}-f) exerts antitumor effects in mouse xenograft models of pancreatic carcinoma. Biochem Biophys Rep 24: 100826, 2020.
72. Ishikawa A, Waseda M, Ishii T, Kaneko MK, Kato Y and Kaneko S: Improved anti-solid tumor response by humanized anti-podoplanin chimeric antigen receptor transduced human cytotoxic T cells in an animal model. Genes Cells 27: 549-558, 2022.
73. Chalise L, Kato A, Ohno M, Maeda S, Yamamichi A, Kuramitsu S, Shiina S, Takahashi H, Ozone S, Yamaguchi J, *et al*: Efficacy of cancer-specific anti-podoplanin CAR-T cells and oncolytic herpes virus G47Δ combination therapy against glioblastoma. Mol Ther Oncolytics 26: 265-274, 2022.
74. Shiina S, Ohno M, Ohka F, Kuramitsu S, Yamamichi A, Kato A, Motomura K, Tanahashi K, Yamamoto T, Watanabe R, *et al*: CAR T cells targeting podoplanin reduce orthotopic glioblastomas in mouse brains. Cancer Immunol Res 4: 259-268, 2016.